Analysis of Surface Black Carbon Distributions during ACE Asia using a Regional Scale Aerosol Model

Itsushi Uno[1)] , Gregory R. Carmichael[2)] , David Streets[3)],
Shinsuke Satake[1)], Toshihiko Takemura[1)], Jung-Hun Woo[2)],
Mitsuo Uematsu[4)] and Sachio Ohta[5]

1: Research Institute for Applied Mechanics, Kyushu University, Kasuga Park 6-1, Kasuga, Japan
2: Center for Global and Regional Environmental Research, University of Iowa, Iowa City, Iowa, U.S.A.
3: Decision and Information Science Division, Argonne National Laboratory, Argonne, Illinois, U.S.A.
4: Ocean Research Institute, University of Tokyo, Tokyo, Japan
5: Faculty of Engineering, Hokkaido University, Sapporo, Japan

(submitted to J. Geophysical Research on 30 Nov. 2002; revised on 14 Feb. 2003)

Corresponding author address:
Itsushi UNO, Research Institute for Applied Mechanics, Kyushu University, Kasuga Park 6-1, Kasuga, Fukuoka 816-8580, Japan (e-mail: iuno@riam.kyushu-u.ac.jp)

Abstract

The regional scale aerosol transport model (CFORS) is used in the analysis of black carbon (BC) observed at 5 remote Japanese islands during the ACE-Asia experiment. BC is modeled on-line in the regional scale meteorological model (RAMS), using emissions estimates for 2000. Two model experiments are conducted 1) a control run that includes all the BC emission; and 2) a sensitivity run without open biomass burning emissions to clarify the impact of biomass burning on the BC levels in the western Pacific. The regional aerosol model (CFORS) is shown to accurately reproduce many of the important features observed. Model analysis shows that the spatial and temporal distributions of black carbon between the northern sites (Rishiri and Sado; located in the Japan Sea) and the southern stations (Hachijo, Chichijima and Amami-Oshima; in the western Pacific Ocean) are under different flow regimes. It is shown that the major synoptic features controlling BC levels are associated with outflow in the warm

conveyor belt of traveling cold fronts, and the subsequent post-frontal transport. At the northern stations (Rishiri and Sado), elevated BC concentrations are calculated to be mainly below the heights of 2,000 m, and the biomass burning fraction is estimated to be below 20%. At the southern sites (e.g., Chichijima), the contribution due to biomass burning reaches 32% at the surface and 52% in the free atmosphere. CFORS results indicate that the major black carbon source and transport height are different between the northern and southern sites.

AGU Index code number: 0305 Aerosols and particles, 0322 Constitutent sources and sink, 0345 Pollution-urban and regional, 0365 Troposphere-composition and chemistry, 3337 Numerical modeling and data assimilation

1. Introduction

Black carbon (BC; also known as elemental carbon, or EC) is the primary absorbing aerosol in the atmosphere [*Liousse et al., 1996; Penner et al., 1993; Cooke and Wilson, 1996*]. It has been estimated by the IPCC that the global mean clear-sky radiative forcing of BC is about + 0.4-0.8 W m^{-2} [IPCC, 2001]. BC also affects cloud albedo and cloud formation. In addition the solar heating caused by BC has been shown to reduce cloudiness [*Ackerman et al., 2000; Kaufman et al., 2002*]. Therefore BC must be considered as one of the key aerosols that control the global climate system.

Several numerical transport modeling studies of carbonaceous aerosol have been reported for the global scale [e.g., *Cook and Wilson, 1996; Liousse et al., 1996; Takemura et al, 2000*] and for regional scale [*e.g., Jacobson 1997; Pai et al, 2000*]. These studies provide important insights into the budget of BC, and point out major uncertainties in sources and sinks, and the limited amount of data upon which to test the model results. Regional scale observational and modeling studies are required to update our understanding of the behavior of carbonaceous aerosol and its radiative impacts on global and regional scales.

Observations in South Asia during the INDOX experiment [*Ramanathan et al., 2001*] revealed a large brown cloud layer (haze) over the Indian Ocean arising from anthropogenic and biomass burning sources. They have shown that the existence of this brown cloud has important impacts on the regional energy balance.

Jacobson [1997] pointed out the importance of aerosols containing BC and OC on regional heating and temperatures, and that these aerosols can significantly affect day- and nighttime temperatures, irradiance, and heating rates. The major black carbon emission sources in Asia are from the residential sector and 'open' biomass burning [*Streets et al., 2002*]. However, the emission rates and the transport processes of BC over East Asia and the western Pacific are not well characterized.

The Asian-Pacific Regional Aerosol Characterization Experiment (ACE-Asia) field study [*Huebert et al., 2002*] was conducted in March, April, and May of 2001 in the vicinity of Japan, Korea, China, and Chinese Taipei. During ACE-Asia BC was measured on aircraft, ships and at several ground sites. These data provide a basis to evaluate and refine models of Asian aerosols and their radiative impact.

As a contribution to the ACE-Asia campaign, we developed a regional scale

chemical transport modeling, chemical weather forecasting system CFORS [*Uno et al., 2002*], and applied the model to help understand the source, transport and deposition processes of Asian aerosol, including mineral dust, sulfate and carbonaceous aerosols. In this paper, we focus on the model evaluation based on the surface black carbon measurements. We investigate the spatial and temporal distributions of black carbon and discuss the outflow patterns of polluted air masses over the western North Pacific during the ACE-Asia period.

2. Carbonaceous Aerosol Measurements

Intensive measurement data are necessary to evaluate our ability to model BC. During ACE Asia, BC was measured at 5 islands around Japan as part of the Variability of Marine Aerosol Properties (VMAP) project [*Uematsu et al.*, 2002; *Matsumoto et al*., *2002a, 2002b*] and the APEX (Asian Atmospheric Particle Environmental Change Studies) project [*Ohta et al., 2002*]. This network consisted of four sites on the Japanese islands of Rishiri, Sado, Hachijo and Chichi-jima. The observation sites are shown in Figure 1, and are distributed in latitude from 25^{o}N to 45^{o}N along the longitudinal line of 140^{o}E. VMAP provides important surface measurements of aerosol composition (elemental and organic carbons, major ions, trace metals and number concentration) and trace gases (SO_2, O_3, CO and radon). Details of the sampling protocol and chemical analysis are reported in *Matsumoto et al.* [2002b].

The concentrations of particulate elemental carbon (EC) were continuously measured by a thermal analysis method using ambient carbon particulate monitors (Rupprecht & Patashnick Co. Inc., Model 5400) at 4-hour intervals on the four islands. Only ambient aerosols with diameter < 2.5μm were introduced into the instrument using a PM2.5 cyclone (with a 50% cutoff efficiency for 2.5μm particles) to eliminate coarse particles. The amounts of carbonaceous substances evolved at 340°C and 750°C were defined as organic carbon (OC) and total carbon (TC), respectively. The difference between the amounts of TC and OC gives the amount of EC. A detailed explanation of the instrument employed in this study was reported in *Uematsu et al.[2001*].

Independent from the VMAP network, surface observations at Amami-Oshima island were conducted under the APEX project [*Ohta et al., 2002*]. At this site, fine particles were sampled on quartz fiber filters (Pallflex 2500QAT-UP, 47mm) and Teflon filters (Sumitomo Fluoropore FP-1000, 47mm). The sample air inlet was 5 m

above the roof and branched into two lines. Each line was connected to a cyclone separator with a 50% cutoff diameter of 2μm. The carbon content in the quartz fiber filter samples were determined by a combustion technique at 850°C in an NC-analyzer (Sumitomo Chemical, Sumigragh NC-80) and the evolved gases were analyzed using gas chromatography (Shimadzu, GC-14A) with a Ni catalyst methanizer and flame ionization detector (FID) [*Ohta and Okita, 1984*]. A portion of the filter was used to determine the total carbon content (TC), and another portion was heated in an electric furnace at 300°C in ambient air for 30 minutes to remove organic carbon (OC) and then used to determine the elemental carbon content (EC). The difference between TC and EC gives the amount of OC. At this site, daily averaged carbonaceous aerosol measurements (averaged from 1000LST to 1000LST of next day) were obtained.

Table 1 shows the location and the averaged BC concentration for each site. These fine particle mode data of BC (PM2.5) were used for the analysis with the CFORS model.

3. BC Transport Modeling : CFORS

Black carbon transport was simulated by the Chemical weather FORecasting System CFORS developed by *Uno et al.* [2002]. CFORS is a multi-tracer, on-line, system built within the RAMS (Regional Atmospheric Modeling System) mesoscale meteorological model [*Pielke et al., 1992*]. An important feature of CFORS is that multiple tracers are run on-line in RAMS, so that all the on-line meteorological information such as 3-D winds, boundary-layer turbulence, surface fluxes, cumulus convection and precipitation amount are directly used by the tracer model at every time step. The technical details of CFORS and general model performance information during the ACE-Asia observation period are reported in *Uno et al.* [2002], and for the TRACE-P (Transport and Chemical Evolution over the Pacific) experiment in *Carmichael et al.* [2002]. Here we will describe some details of the black carbon transport module within CFORS.

We assumed that black carbon exists solely in the fine mode, and in the results presented here we ignored gravitational settling, wet deposition, and chemical aging processes. Dry deposition velocities were set at 10^{-4} (10^{-3}) m sec^{-1} for ocean (land) surfaces. Cumulus convection plays an important role for the vertical distribution of biomass burning BC sources in subtropical regions, such as southern China, Thailand

and Myanmar. The vertical redistribution of tracers by cumulus activities was treated as enhanced vertical turbulent diffusivities from the bottom to top of the cumulus cloud layers as identified by the RAMS simplified Kuo cumulus scheme [*Tremback, 1990*].

Figure 1 shows the numerical model domain of CFORS, which is centered at 25˚N and 115˚E on a rotated polar-stereographic projection. The horizontal grid consists of 100 by 90 grid points, with a resolution of 80 km. The model's vertical domain extends from surface to 23km with 23 non-uniform grids varying from 150 m thick at the surface to 1800 m thick at the top.

Figure 1 also shows the black carbon emission distribution from (a) anthropogenic (including biofuel) and (b) open biomass burning sources (unit is $\mu g/m^2/sec$). The solid dot symbols indicate the surface observation sites from VMAP (R:Rishiri, S;Sado, H:Hachijo and C:Chichijima islands) and APEX (A:Amami-Oshima island) networks. The black carbon emission inventory was based on Streets *et al*.[2002] and is described in the next section. In Figure 1(b), we also shows the model calculated total precipitation amount (mm/2 months) by the blue contour lines.

The CFORS chemical transport calculation in the post-analysis mode was conducted for the period February 20, 2001 through May 31, 2001 with a zero initial BC concentration. The ECMWF (European Center for Mid-range Weather Forecast) global meteorological data set (6 hour interval with 1˚×1˚ resolution), analyzed weekly SST (sea surface temperature) data, and observed monthly snow-cover information were used as the boundary conditions for the RAMS calculation. Two numerical experiments were conducted: 1) a control run (CNTL) that includes all the BC emissions; and 2) a sensitivity run (BOFF) without biomass burning emissions to clarify the impact of biomass burning on the BC levels in the western Pacific.

4. BC Emissions

Black carbon emissions developed by *Streets et al*. [2002] were used in this study. This inventory was designed to survey air pollutant emissions for Asia for the year 2000, and to conduct modeling analysis in support of the NASA TRACE-P, the NSF/NOAA ACE-Asia, and the NOAA ITCT 2K2 experiments. The domain studied stretches from Pakistan to Japan, and from Indonesia to Mongolia.

Anthropogenic BC emissions were estimated for various sectors including industry, domestic (including combustion of biofuels, such as wood, crop residues, and

dung), transport, power generation and agricultural. BC emission from "open" burning (forest burning, savanna/grassland burning, and the burning of crop residues in the field after harvest) were estimated separately. Because biomass burning has important day-to-day variations due to local agricultural practices and precipitation amounts, daily emissions were estimated. Monthly emissions were calculated for each region based on statistics of the type and amounts of biomass burned. These monthly amounts were then parsed into gridded daily emissions using AVHRR satellite fire counts [*Streets et al., 2002*].

The resulting BC emissions due to energy and open burning are presented in Figure 1. Annual total black carbon emissions in Asia are estimated to be 2.54 Tg. It is important to notice that the fraction from biomass burning and the residential sector occupies 18 % and 64% of annual emission, respectively [*Streets et al., 2002*]. The total anthropogenic black carbon emissions in the CFORS domain between March and April are estimated to be 0.29 Tg, while the total emissions from biomass burning were 0.17 Tg. (Note that Figure 1b shows the averaged BC emission based on the daily emission amount). March and April is the highest season of 'open' burning in the Indo-China peninsula.

5. Results and Discussion

a) Time variation of BC concentration

Figure 2 shows the time variation of simulated BC concentrations at the 5 sites. The red open circles indicate the observations, the solid line indicates the CNTL simulation, the dashed line represents the BOFF simulation (i.e., without biomass burning emission), and the dot-broken line is the CFORS-calculated wind direction at z=500m. The thick blue line is the daily precipitation amount from the nearest observation station (AMeDAS) operated by the Japan Meteorological Agency. Note that the solid star symbols in Figure 2(e) indicate the scaled concentration between observation and model (discussed later). Summaries of the comparison between the observed and simulated concentrations and precipitation amount are shown in Table 1. In this table the biomass fraction (BIOfrac) is calculated by

$$\text{BIOfrac} = (BC_{CNTL} - BC_{BOFF}) / BC_{CNTL} * 100\ (\%) \qquad (1)$$

When compared against the averaged values during the observation periods (values in parenthesis in the CFORS column in Table 1), the modeled values are within 40% of the

observed value. In addition the model predictions identify correctly the locations with the highest values (Sado, Amami-Oshima) as well as the lowest values (Chichijima).

Further details are found by examining the time-series at each site (Figure 2). As shown in Figure 2, the model results are generally in very good agreement with the observations and can explain the absolute concentration levels and much of the variation with time. One important feature is the intermittent outflow of pollutants from the Asian continent that is observed and also simulated at Rishiri and Sado. The time variation at these sites is synchronized, indicating that these two islands are controlled by similar synoptic weather systems. During this period the major synoptic features controlling BC levels are associated with outflow in the warm conveyor belt of the traveling cold fronts, and the subsequent post-frontal transport. The role of these transport features in determining surface distributions have been discussed previously [e.g., *Uno et al., 2000, 2001*; *Kaneyasu et al., 2000*]. The VMAP BC observations confirm that these weather systems often activate the outflow of polluted BC-air masses to the northwestern Pacific.

The time variation in BC at Hachijo, Chichijima, and Amami-Oshima exhibit similar features, but which are different from those at the northern two sites. For example, at the northern sites the BC levels increase dramatically during the Julian days 115-120, while the concentrations at the southern sites decrease during this period. Another important feature, is that the values at Amami-Oshima are substantially higher than those observed at the other sites. It is well known that carbonaceous aerosol analysis is very sensitive to the chemical analysis method. The BC analysis method between the VMAP and the APEX sites are different, and there is the possibility of systematic bias between them. To explore this possibility further, we calculated a scaled BC concentration at Amami-Oshima, based on a regression analysis between the observations at Hachijo, Chichijima and Amami-Oshima. We found that the observations between these three sites were correlated, but that the values at Amami-Oshima were systematically high. The values at Amami-Oshima could be scaled to be consistent with the values at the other sites using the model: $y_{scaled} = 0.4BC_{obs\text{-}Amami} + 0.2$. This regression indicates that the differences between the analytical techniques themselves may lead to a factor of 2 difference in the observed values. The resulting ‘scaled observation data’ is shown by the solid star symbols in Figure 2e. When we compare the model simulation with the scaled observation data, it is clear that the model

reproduces the fundamental daily variation, and that the time variation is very similar to that observed at Hachijo. Clearly more work is needed to standardize BC analysis.

Simulated BC at Sado is sometimes systematically under predicted. This happens between Julian days of 96-102, 108-110 and 116-121. During these periods, the wind direction was mainly from east to south, implying that BC concentrations are predicted low when the air masses are coming from Japan. Sado is located 30 km northwest of the Japanese main island, and the observed levels of BC must have a strong influence from Japanese sources under these flow conditions. This suggests that BC emissions from Japan may be under-estimated in April. One possible cause is that biomass burning emissions (associated with agricultural waste before rice-planting season) may be underestimated. The local biomass burning is highly uncertain and needs more careful examination to identify the possible sources of BC during this season in Japan.

It is important to point out that the model sometimes over-predicts BC; e.g., at Rishiri (Day 93), Hachijo (Day 91) and Chichijima (Jday 97-99). On these days, the JMA observation (AMeDAS) and RAMS model show relatively strong precipitation. This indicates that the washout of BC may be important. The northern side of the model domain (latitude higher than approximately 35˚N) had less precipitation (see Figures 1(b) and 2), so the modeled BC explained the observational variation of BC very well. Most of the precipitation at Rishiri and Hachijo in the spring result from cold front activities. The transport of BC high concentration from Asian Continent is associated with the post frontal outflow. Therefore the precipitation event in Rishiri (Jday 93) and Hachijo (Jday 91) also brought relatively high levels of BC, and that the wash out process becomes important.

On the other hand, as shown in Table 1, the RAMS precipitation amount in the southern part of the domain is under estimated (note that the RAMS model reproduced the rain events correctly). Over the region from Taiwan to the south of the Japanese main island, precipitation amounts of 200-300 mm/(2 months) occur in association with the spring rain belts. The southern VMAP measurement sites sometimes observed heavy precipitation. Figure 2 shows that the model results reproduced the observed BC variation during the no precipitation periods. Figure 2 also shows that the model results agree with the observations even during the precipitation events. This is because the observed BC is highly dependent on the accumulated wet removable along the

transport path, as well as the distribution of BC emission sources. Clearly further work on modeling BC removal is needed.

b) Time-Height Profile of Black Carbon

Figure 3 shows the time-height cross-sections of BC for the 5 island sites. In this figure the contour lines indicate the BC concentration, while the color shading reflects the fraction of the BC due to biomass burning emissions (BIOfrac). The time-height profiles of BC have interesting characteristics, and illustrate the fact that surface observations do not always capture the maximum BC levels. At Rishiri and Sado, elevated BC concentrations are calculated to be mainly below heights of 2000 m. Furthermore, the biomass burning fraction (BIOfrac) is below 20% at these sites. At Amami-Oshima and Chichijima, elevated BC layers are often calculated. The BIOfrac values shown in Table 1 and Figures 2 and 3, are large at the southern sites. For example, the surface (column) BIOfrac at Chichijima is 32% (52%), while at the most northern station of Rishiri it is 16% (19%). The large BIOfrac at the southern sites is due to the fact that the biomass burning sources are mainly located in southern China and the Indo-China peninsula (shown in Figure 1(b)). Emissions from these areas are transported off the continent in the warm sector of the cold fronts that sweep over east Asia in the springtime. As discussed in *Tang et al*. [2002], the flux of biomass pollutants is largest in the latitude belt of 15-25˚N, and at altitudes of 2-4 km. Thus the southern island sites are well positioned to see biomass BC in the springtime.

Large contributions due to biomass burning were simulated between Julian day 69-72, 75-82 and 84-88 at Amami-Oshima, Chichijima and Hachijo. Back trajectory analysis of these elevated biomass layer (not shown in Figure) indicate that the main source region was in south-east Asia (such as Thailand and Myanmar). During these periods, the TRACE-P air borne campaign observed elevated CO layers in the free atmosphere, and the main sources of these CO plumes were identified to originate in south-east Asia [*e.g., Carmichael et al., 2002; Zhang et al, 2002*]. These results indicate that the major black carbon source and transport height are different between the northern and southern regions of the VMAP sites.

c) Case studies of BC outflows

Further insights can be found by looking in detail at specific transport events.

Figure 4 shows the surface level BC concentrations and near surface winds for (a) March 20, 2001, (b) March 21, 2001, (c) April 9, 2001 and (d) April 11, 2001.

During March 18 to 23, a large scale pollution belt existed from southeast Asia to Japan [*Zhang et al., 2002*]. Elevated BC occurred over all the surface stations. On March 20 (Julian Day 79), the region from Shanghai – Korean peninsula – Japan island was located within the warm sector of a low-pressure system, and the surface winds were from the SW. A large cold front extended from Bejing to eastern Siberia. At this time a polluted air mass, with BC concentrations higher than 1.5 $\mu g/m^3$, was located over the Japan Sea. This polluted air mass arrived at Rishiri and Sado on March 20. By March 21, the main body of the elevated BC air mass had passed over Rishiri and Sado, and concentrations decreased in the air mass behind the cold front. This outflow event influenced all 5 sites. As shown in Figures 4 and 3, the northern sites were influenced by anthropogenic emissions and the southern sites by biomass burning.

The episode from April 8 to 12 (Julian Days 98-102) was different from the one discussed above. During the period a cold front was located northwest of Beijing on April 9, and a large traveling low pressure system was moving to the east from the north-east of Taiwan to the south of Tokyo (towards Hachijo). The counter-clockwise easterly winds brought relatively clean Pacific air, with low BC concentrations, to Hachijo, Chichijima, and Amami-Oshima. In contrast, at Sado the winds were S to SE bringing high BC concentrations from Japan. At Rishiri, the BC concentrations gradually increased due to the warm sector transport (SW wind), and then suddenly showed a rapid decrease on April 12 (after the passage of the cold front). As the traveling low-pressure system moved to the east, the BC polluted front covered Amami-Oshima and Hachijo (April 11 – 12th(Day 101-102)). Model results show that the pollution front arrived first at Chichijima (April 10) and then at Amami, approximately 8 hours before arriving at Hachijo. The early arrival of the BC front at Chichijima (April 10) is due to warm sector transport just south of the moving low-pressure system.

These two episodes indicate that the mechanisms controlling the outflow of BC from the Asian continent have distinct differences within the 2000km separating the northern and southern latitude of the VMAP networks.

d) Monthly averaged concentrations and transport fluxes

The discussions above illustrate: (i) the differences in time variations between

the Rishiri-Sado sites and Hachijo-Chichijima-Amami sites; (ii) a significant south-north concentration gradient; (iii) the biomass burning contribution for BC is higher at the southern sites; and (iv) there are elevated layers of BC that are decoupled from the surface. These results demonstrate that the transport patterns of BC-polluted air masses from the East Asian continent to the Japan and the northern Pacific are often different from those to the southern regions.

Figure 5 shows the two-month (March and April) averaged BC fields. Figure 5(a) shows the averaged surface concentration (by line), the biomass burning BC fraction (BIOfrac) in color, and the horizontal transport flux ($HFLX_x$, $HFLX_y$) by vector. Figure 5(b) shows the column-averaged fluxes. Here the horizontal transport flux is calculated by,

$$HFLX_x = \frac{1}{T}\int^T u \times C_{BC}\, dt, \quad HFLX_y = \frac{1}{T}\int^T v \times C_{BC}\, dt \qquad (2)$$

where, u and v are the wind speed in the x, y directions; C_{BC} is the black carbon concentration; and T is the averaging period (March and April).

Surface level BC concentrations are highest in the central China (>2 $\mu g/m^3$). At the measurement sites the simulated concentrations are highest at Amami (0.6 $\mu g/m^3$), then Sado (0.55$\mu g/m^3$), and Hachijo (0.5$\mu g/m^3$). The averaged values at Rishiri and Chichijima are lower and almost the same (0.35$\mu g/m^3$). As shown in Table 1, the calculated concentrations are consistent with the observed averages as discussed previously.

Along the longitude line of 140˚E, the concentration peak is located just to the south of Sado. The south-north concentration gradient is estimated to be ~0.17$\mu g/m^3$/1000km. The west-east concentration gradient between Amami-Oshima and Sado is ~0.18$\mu g/m^3$/1000km. This indicates that the concentration gradient over Japan is essentially the same magnitude in both directions.

The mean surface horizontal transport pattern shows a clockwise flow pattern, with the flow center located over central China. The horizontal flux over Korea and Japan is in the NE direction, while it is SW in Taiwan and southern China. The transport patterns in the northern areas indicate that anthropogenic emission are mainly transported in the direction of Sado and Rishiri. Under these conditions the biomass burning fraction is approximately 15%. The contribution of biomass burning in the Indo-China outflow exceeds 80%. These results also identify that the Amami-Oshima

site is located at the split point of the horizontal transport flux streamline (separating easterly from southerly outflow), and that Amami-Oshima and Chichijima are located on the same streamline of the horizontal BC transport flux.

The column averaged BC concentration field is similar to the surface values. However, the column averaged horizontal transport direction is quite different from the surface layer. Because of the strong westerly flows and the intensive biomass burning in SE Asia, the main horizontal transport direction is from Indo-China – to the south of Japan. The southern stations at Hachijo, Amami-Oshima and Chichijima are strongly influenced by biomass burning. Clarke *et al.*[2002] show that the biomass BC fraction is higher in the free atmosphere at the latitudes lower than 25˚N during TRACE-P. This observational fact is consistent with the results of Figure 3.

Because the VMAP observations were located approximately along the longitude of 140˚E, the averaged vertical concentration field along 140˚E is of interest. Figure 6 shows: (a) the averaged concentration by color and BIOfrac by line; and (b) the averaged HFL_X by color and biomass fraction of HFL_X by line. Figure 7 shows the averaged vertical profiles at the 5 sites. High black carbon concentration are calculated below 2km, and the vertical profile pattern is very sharp over the northern sites of Sado and Rishiri (see Figure 7). Within the free atmosphere, the highest concentrations are simulated at Amami-Oshima, and levels at Chichijima are higher than at Hachijo. This is clearly shown in Figure 7.

The horizontal transport flux has two peak regions, one in the boundary layer between 36˚N – 44˚N (BIOfrac of 15-20%), and the other in the free atmosphere between 26˚N – 32˚N (BIOfrac of 50-60 %). The transport mass flux within the BL is mainly due to anthropogenic emissions and transported by synoptic weather patterns, while the upper level flux is dominated by biomass burning emissions transported in the strong westerlies associated with the warm conveyor belt [*Carmichael et al., 2002*]. As we can see from Figure 6b, there is a strong latitudinal gradient of BIOfrac (~2.5%/deg).

5. Conclusions

During the ACE-Asia experiment, high time resolution BC observations were made at 5 isolated Japanese islands under the projects of VMAP [*Matsumoto et al., 2002a*] and APEX [*Ohta et al, 2002*]. These measurements provide a data set to

examine the time variation and horizontal distribution of carbonaceous aerosol. The regional scale aerosol transport model (CFORS) was used in the analysis of these surface observations. The regional scale meteorological model (RAMS) provided a means to produce dynamic flow fields with high space and time resolution. BC was calculated on-line using the emission inventories developed by Streets *et al*. [2002]. Two model experiments were conducted 1) a control run (CNTL) that includes all the BC emission; and 2) sensitivity run (BOFF) without open biomass burning emissions to clarify the impact of biomass burning on the BC levels in the western Pacific.

A detailed analysis of the modeled and observed BC values was performed, with emphasis on the spatial and temporal distributions of black carbon, the outflow patterns of polluted air masses over the western North Pacific, the contribution of biomass burning, and the horizontal transport flux during the ACE-Asia period. We found that:

1) The two northern stations (Rishiri and Sado islands) show an intermittent outflow of pollutants from the Asian continent. The time variation at these sites is synchronized, indicating that these two islands are controlled by similar synoptic weather systems. The major synoptic features controlling BC levels are associated outflow in the warm conveyor belt of traveling cold fronts, and the subsequent post-frontal transport. The three southern stations (Hachijo, Chichijima, and Amami-Oshima) show time variations in BC which are similar, but which are different from those at the northern two sites.

2) At Rishiri and Sado, elevated BC concentrations are calculated to be mainly below the height of 2,000 m. The biomass burning fraction (BIOfrac) is below 20% at these sites. The BIOfrac at Chichijima had a maximum value of 32% at the surface and 52% in the free atmosphere. This large BIOfrac at the southern sites reflects the fact that the biomass burning sources are mainly located in southern China and the Indo-China peninsula. Large contributions due to biomass burning were simulated between Julian day 69-72, 75-82 and 84-88 at Amami-Oshima, Chichijima and Hachijo. Back trajectory analysis indicates that the main source region of these elevated BC is in south-east Asia (such as Thailand and Myanmar). CFORS sensitivity results indicate that the major black carbon source and transport

height are different between the northern and southern regions of the VMAP network.

3) Analysis of the two-month averaged concentration fields and the transport patterns helped explain the surface level BC concentration distributions. At the measurement sites the simulated concentrations are highest at Amami (0.6 $\mu g/m^3$), then Sado (0.55$\mu g/m^3$), and Hachijo (0.5$\mu g/m^3$). The surface horizontal transport patterns show a clockwise flow pattern, with the flow center located over central China. The horizontal flux over Korea and Japan is in the NE direction, while it is SW in Taiwan and southern China. The transport patterns in the northern areas indicate that anthropogenic emissions are mainly transported towards Sado and Rishiri. The column averaged BC concentration fields are similar to the surface values. However, the column averaged horizontal transport direction is quite different from the surface layer. The southern stations of Hachijo, Amami-Oshima and Chichijima are strongly influenced by biomass burning.

4) The horizontal transport flux at 140˚E has two peak regions, one in the boundary layer between 36˚N – 44˚N (BIOfrac of 15-20%), the other in the free atmosphere between 26˚N – 32˚N (BIOfrac of 50-60 %). The transport mass flux within the BL is mainly due to anthropogenic emissions and transported by synoptic weather patterns while the upper level flux is dominated by biomass burning emissions transported in the strong westerlies.

Based on the results presented in this paper, it appears that the emission estimates of BC are qualitatively correct. This statement is based on the fact that the calculated values at the four VMAP sites are consistent with the observations. There is also an indication that the emissions from Japan may be underestimated, and that this may be associated with local biomass burning of agriculture waste. Analysis of the CFORS calculations of the TRACE-P aircraft data for BC led to a similar conclusion, but pointed out a systematic problem in under predicting BC levels at low altitudes in the Yellow Sea [*Carmichael et al.,* 2002]. Therefore the above statements regarding BC emissions are preliminary, especially in light of the fact that reported BC values are very dependent on the analysis method.

Clearly more work is needed to better quantify BC distributions in East Asia. One important topic is related to how best to use the surface data in the constraint of BC emission estimates. This is particular difficult as much of the flux of BC occurs at altitudes well above the surface layer. Another important issue that needs to be addressed before quantitative statements regarding BC emissions can be made is related to the deposition fluxes of BC. At present we do not have sufficient information upon which to constrain wet and dry removal fluxes of BC. However, results presented in this paper suggest that wet removal of BC influences the surface time-series, and that further work on modeling BC removal is needed in our model. We plan to address these issues, along with an analysis of the BC aircraft data obtained in AceAsia, in a subsequent paper.

Acknowledgements

This work was partly supported by Research and Development Applying Advanced Computational Science and Technology (ACT-JST) and Core Research for Evolution Science and Technology (CREST) of Japan Science and Technology Corporation (JST). This work (G.R.Carmichael and D. Streets) was also supported in part by grants from the NSF Atmospheric Chemistry Program and the NASA ACMAP and GTE programs.

References

Akerman,A.S., O.B. Toon, D.E.Stevens, A.J. Heymsfield, V.Ramanathan and E.J. Welton, Reduction of tropoical cloudniss by soot, *Science*, **288**, 1042-1047, 2000.

Clarke, A., S. Howell, S. Masonis, R. Weber, V. Kapustin, C. McNaughton and K. Moore, Aerosol microphysics, chemistry, optical properties and humidity growth in Asian outflow, CACGP/IGAC Joint International Symposium on Atmospheric Chemistry within the Earth System, p. 167, Crete, Greece, 2002.

Carmichael,G.R., Y. Tang, G. Kurata, I. Uno et al., Regional-scale chemical transport modeling in support of intensive field experiments: Overview and analysis of the TRACE-P Observations, submitted to *J. Geophys. Res.,* 2002.

Cooke, W.F., Wilson, J.N., A global black carbon aerosol model. *J. Geophys. Res.,* **101**, 19, 395-19,409, 1996.

Huebert, B., T. Bates, P. Russell, G. Shi, Y.J. Kim, and K. Kawamura, An overview of

ACE-Asia: strategies for quantifying the relationships between Asian aerosols and their climatic impacts, to be submitted *J. Geophys. Res.,* 2002.

IPCC (the Intergovernmental Panel on Climate Change), *Climate Change 2001: The Scientific Basis*, J. T. Houghton, Y. Ding, D. J. Griggs, M. Noguer, P. J. van der Linden, D. Xiaosu, K. Maskell, and C. A. Johnson (Eds.), 896 pp. Cambridge Univ. Press, New York, 2001.

Jacobson, M.Z., Development and application of a new air pollution modeling system – Part III. Aerosol-phase simulations, *Atmos. Enviorn.*, **31**, 587-608, 1997.

Kaufman, Y.J., D. Tanre and O. Boucher, A satellite view of aerosols in the climate system, *Nature*, **419**, 215-223, 2002.

Kaneyasu, N., K. Takeuchi, M. Hayashi, S. Fujita, I. Uno, and H. Sasaki, Outflow patterns of pollutants from East Asia to the North Pacific in the winter monsoon, *J. Geophys. Res.,* **105**, 17361-17377, 2000.

Liousse, C., Penner, J.E., Chuang, C., Walton, J.J., Eddleman, H., Cachier, H., A global three-dimensional model study of carbonaceous aerosols. Journal of Geophysical Research, **101**, 19411-19432, 1996.

Matsumoto, K., M. Uematsu, T. Hayano, K. Yoshioka, H. Tanimoto and T. Iida, Simultaneous measurements of particulate elemental carbon on the ground observation network over the western North Pacific during the ACE-Asia compaign, *J. Geophy. Res.,* 2002a (accepted).

Matsumoto,K., Y. Uyama, T. Hayano, H. Tanimoto, I. Uno and M. Uematsu, Chemical properties and outflow patterns of anthropogenic and dust particles in Rishiri Island during the ACE-Asia campaign. submitted to *J. Geophy. Res.,* 2002b.

Ohta, S. and T. Okita,Measurment of particulate carbon in urban and marine air in Japanese areas. *Atmos. Enviorn.*, **18**, 2439-2445, 1984.

Ohta,S., Kato,R., Murao,N. and Yamagata,S., Measurements of optical and chemical properties of atmospheric aerosols at Fukue and Amami-ohshima island in APEX-E1 and APEX-E2. submitted to *J. Geophy. Res.,* 2002.

Pai, P., K. Vijayaraghavan and C. Seigneur, Particlate matter modeling in the Los Angeles Basin using SAQM-AERO, *J. Air and Waste Manage. Assoc.*, **50**, 32-42, 2000.

Penner, J.E., Eddleman, H., Novakov, T., 1993. Towards the development of a global inventory for black carbon emissions. *Atmospheric Environment,* **27**, 1277-1295.

Pielke,R.A., W.R.Cotton, R.L.Walko, C.J. Tremback, W.A. Lyons, L.D. Grasso, M.E. Nicholls, M.D.Moran, D.A. Wesley, T.J. Lee and J.H. Copeland, A comprehensive meteorological modeling system -RAMS, *Meteorol. Atmos. Phys.*, **49**, 69-91, 1992.

Ramanathan,V. *et al*, Indian Ocean Experiment: An integrated analysis of the climate forcing and effects of the great Indo-Asian haze, *J. Geophy. Res.,* **106**, 28371-28398, 2001.

Streets, D. G., T.C. Bond, G.R.Carmichael, S. Femandes, Q. Fu, D. He, Z.Klimont, S.M.Nelson, N.Y. Tsai, M.Q.Wang, J.-H.Woo and K.F. Yarber, A-year 2000 inventory of gaseous and primary aerosol emission in Asia to support TRACE-P modeling and analysis, sumitted to *J. Geophy. Res.*, 2002.

Takemura,T., H. Okamoto, Y. Maruyama, A. Numaguti, A. Higurashi and T. Nakajima, Global three-dimensional simulation of aerosol optical thickness distribution of various origins, *J. Geophy. Res* **, 105**, 17853-17873, 2000.

Tang, Y., G. Carmichael, J-H Woo, N. Thongboonchoo, G. Kurata, I. Uno, D. Streets, D. Blake, R. Weber, R. Talbot, and H. Singh, The influences of biomass burning during TRACE-P experiment identified by the regional chemical transport model, submitted to *J. Geophys. Res.,* 2002.

Tremback ,C.J., Numerical simulation of a mesoscale convective complex: model development and numerical results, Ph.D. dissertation, Atmos Sci. Paper No. 465, Department of Atmos. Sci., Colorado State Univ., 1990.

Uematsu, M., K. Ohta, K. Matsumoto, and I. Uno, Short term variation of marine organic aerosols under the Northwestern Pacific high pressure region in the summer of 1999, *Geochem. J.,* **35**, 49-57, 2001.

Uematsu *et al*., 2002: http://mits10.ori.u-tokyo.ac.jp/vmap/index.htm

Uno,I., E.-S. Jang, K. Murano, T. Shimohara, O. Oishi, A. Utsunomiya, S. Hatakeyama, Xiaoyan Tang and Yong Pyo Kim, Wintertime intermittent transboundary air pollution overeast Asia simulated by a long-range transport model, *Global Environment Research*, **4**, 3-12, 2000.

Uno,I., H. Amano, S. Emori, K. Kinoshita, I. Matsui and N. Sugimoto: Trans-Pacific Yellow Sand Transport observed in April 1998: Numerical Simulation, *J. Geophy. Research*, **106**, 18331-18344, 2001.

Uno, I., G.R. Carmichael, D. Streets, Y. Tang *et.al.* ; Regional Chemical Weather Forecasting System CFORS: Model Description and Analysis of Surface

Observations at Japanese Island Stations During the ACE-Asia Experiment, submitted to *J. Geophy. Res.,* 2002.

Wang. Y., D.J. Jacob and J.A. Logan, Global simulation of tropospheric O_3-NOx-hydrocarbon chemistry. 1. Model formulation. *J. Geophy. Res.*, **103**, 10,713-10,725, 1998.

Zhang, M., I.Uno, Z. Wang, H. Akimoto, G. R. Carmichael, Y. Tang, J.-H. Woo, D. G. Streets, G. W. Sachse, M. A. Avery, R. J. Weber, and R. W. Talbot, Large-Scale Structure of Trace Gas and Aerosol Distributions over the Western Pacific Ocean during TRACE-P, submitted to *J. Geophy. Res.*, 2002.

Table 1 Observation sites, observed and modeled concentration,the contribution of biomass burning to BC concentrations, and the precipitation amount.

Sites [a]	Longitude Latitude	Observation Period [b]	Observed BC($\mu g/m^3$)	CFORS BC ($\mu g/m^3$)[e]	Biomass Fraction [c]	Precip.[f] (mm)
Rishiri	45.12°N	March 2001	0.36	0.30 (0.36)	16%	27 (44)
	141.20°E	April 2001	0.43	0.41	19%	45 (26)
Sado	38.25°N	March 17-April 30	0.63	0. 53 (0.57)	14%	103(109)
	138.40°E			0.50	20%	18 (7)
Hachijo	33.15°N	March 24-April 30	0.33	0. 57 (0.46)	21%	215 (79)
	139.75°E			0.40	34%	337(183)
Chichijima	27.07°N	March 28-April 30	0.21	0. 37 (0.29)	32%	114 (52)
	142.22°E			0.28	53%	244(165)
Amami -	28.44°N	April 3 – 29	0. 63	0. 72 (0.48)	25%	146(141)
Oshima	129.70°E		0.45 [d]	0.47	47%	376(201)

a) Rishiri, Sado, Hachijo and Chichijima were operated by VMAP project; Amami-Oshima was operated by APEX project.

b) Time resolution at Rishiri, Sado, Hachijo and Chichijima is set to 4 hours, while at Amami-Oshima it is set 24 hours.

c) Fraction of biomass burning origin BC (upper value = for surface concentration; bottom value = for vertically averaged concentration)

d) Scaled concentration ($0.4\ BC_{OBS} + 0.2$)

e) Model simulation average. Upper row is monthly averaged of March, lower row is for Arpil. Value in parenthesis is the average value during the observation period.

f) Surface total precipitation amount (mm). Upper row is monthly total of March, lower row is that of April observed at the nearest Japan Meteorogical Agency's Observation network (AMeDAS) and the value in parenthesis is the RAMS total precipitation.

List of Figures

Figure 1 (a) anthropogenic black carbon emissions ($\mu g/m^2/s$), (b) biomass burning black carbon emissions ($\mu g/m^2/s$) and RAMS calculated total precipitation during March and April (mm) by contour line. Solid dots indicate the observation sites (R: Rishiri, S: Sado, H: Hachijo, C:Chichijima and A:Amami-Oshima islands)

Figure 2 Comparison of time variation of the model (lines) and observation(red symbols). Straight line indicates the control run (CNTL), dashed line for biomass off experiment (BOFF), and light broken line for wind direction. In e) red solid star is scaled concentration using 0.4 BC_{obs_Amami}+0.2. Thick blue line shows the observed daily precipitation by the Japan Meteorological Agency.

Figure 3 Time-height plot of BC concentration (line) and biomass BC fraction (%) by color at the 5 observation sites.

Figure 4 Horizontal distribution of wind field and BC concentration at the surface (z=75m). (a) March 20, (b) March 21, (c) April 9 and (d) April 11, 2001. Contour interval is 0.2 $\mu g/m^3$.

Figure 5 (a) Horizontal distribution of monthly averaged BC concentration ($\mu g/m^3$) by line, biomass burning fraction by color, and horizontal flux ($\mu g/m^2/s$) by vector averaged over March and April. (b) same as (a) but for column averaged concentration field.

Figure 6 Vertical distribution of (a) averaged BC concentration and (b) horizontal transport flux along 140˚E line (averaged over March and April). Biomass burning fraction is shown by line. Characters R, S, H and C are VMAP observation sites.

Figure 7 Vertical profile of monthly averaged BC concentration for 5 observation sites.

a) Anthropogenic BC emission

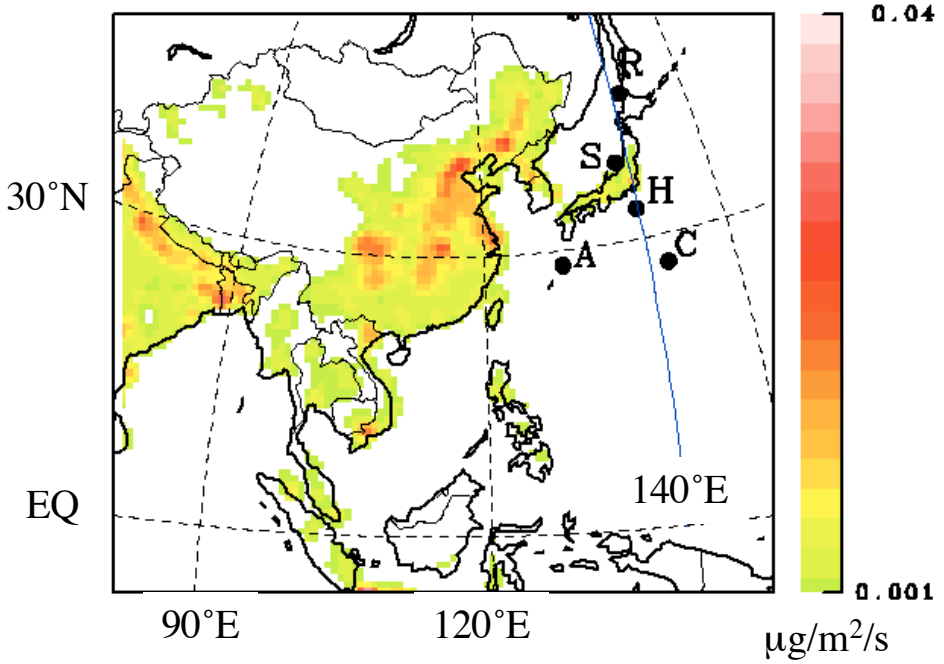

b) Biomass burning BC emission and the RAMS total precipitation

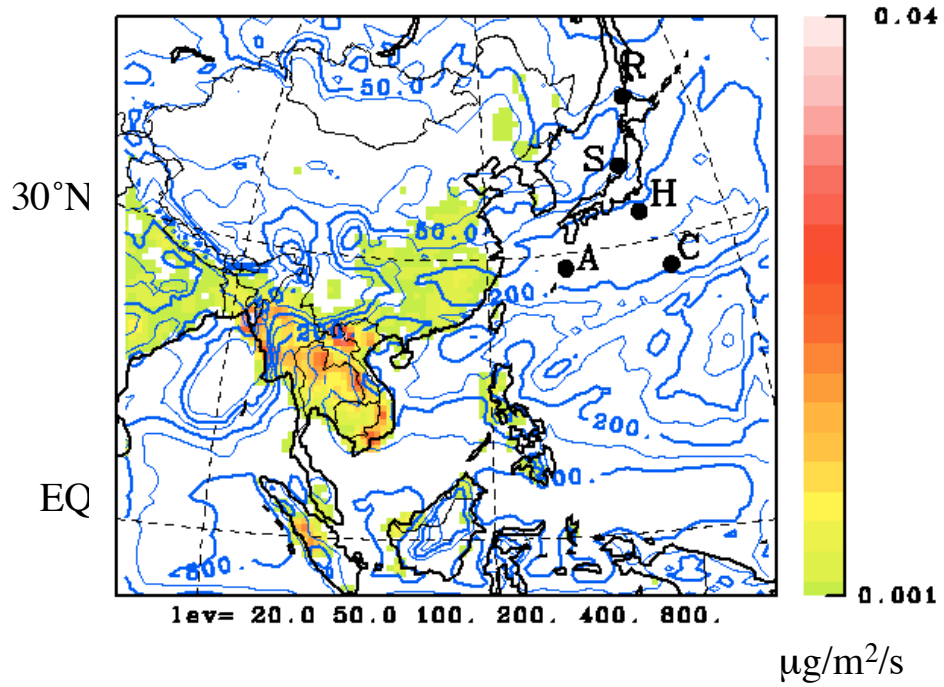

Fig. 1

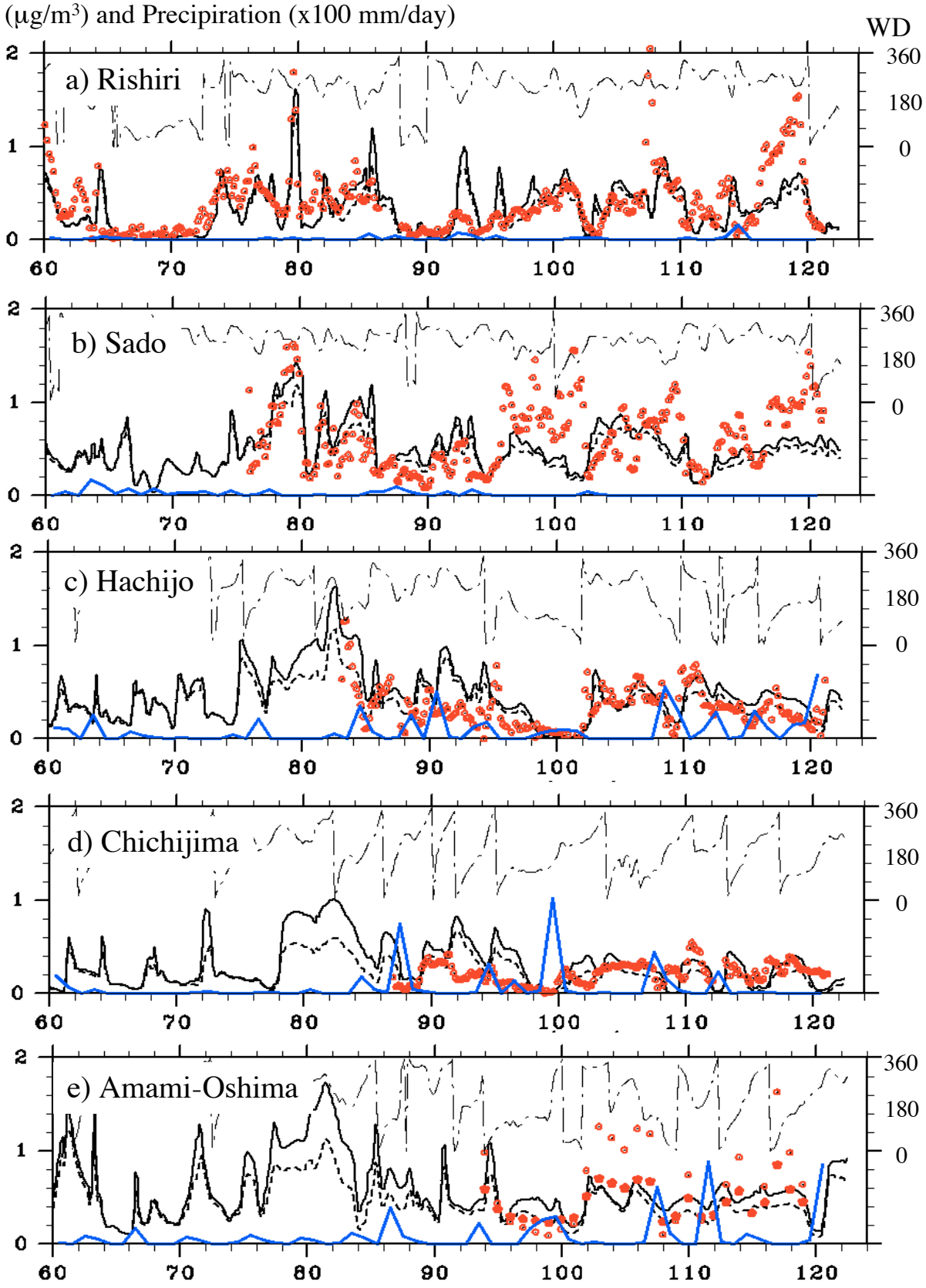
BC (μg/m³) and Precipiration (x100 mm/day)
WD
a) Rishiri
b) Sado
c) Hachijo
d) Chichijima
e) Amami-Oshima
0
1
2
60
70
80
90
100
110
120
360
180
0
Day of Year 2001 (JST)

Fig.2

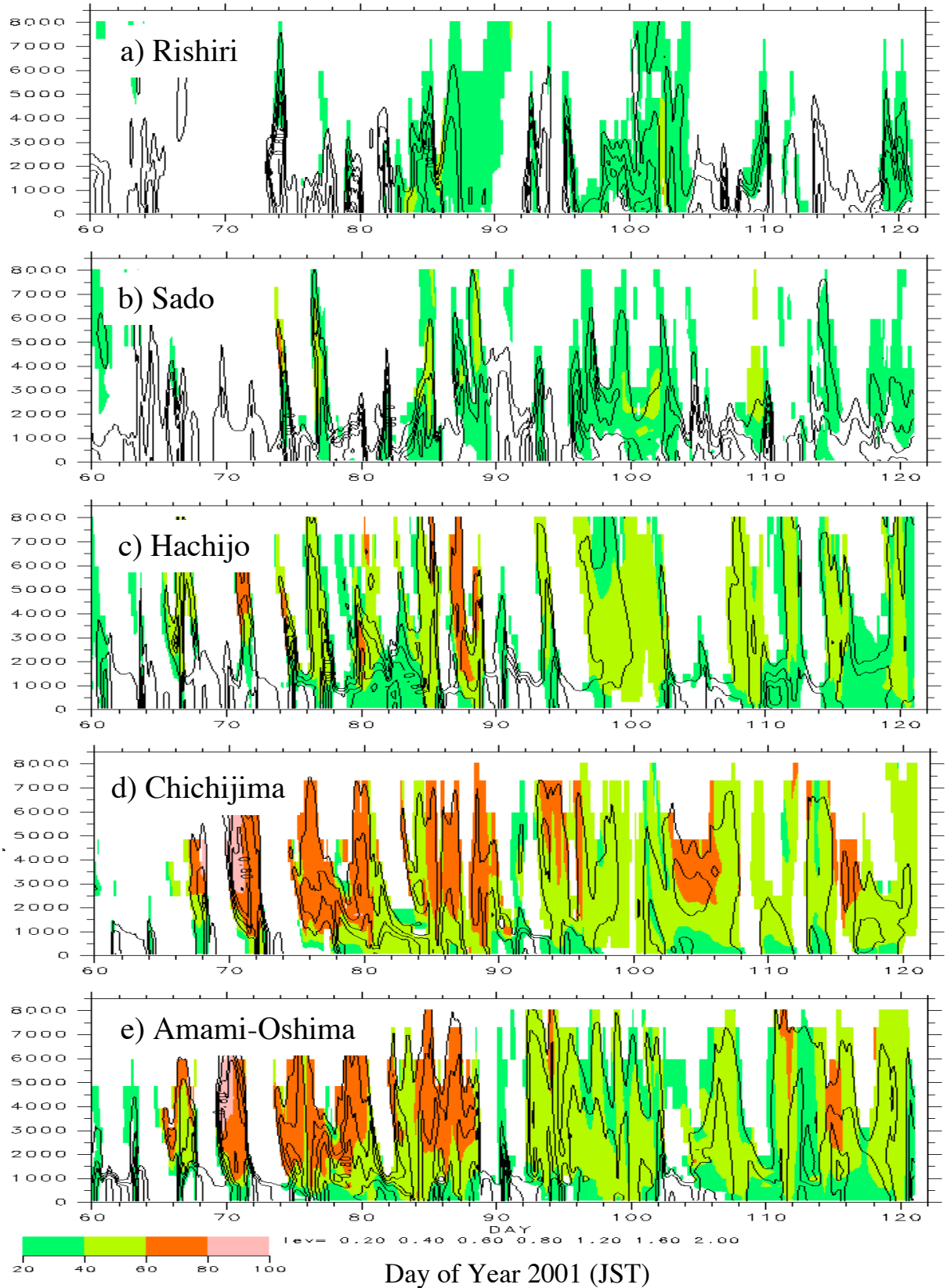
a) Rishiri
b) Sado
c) Hachijo
d) Chichijima
e) Amami-Oshima
8000
7000
6000
5000
4000
3000
2000
1000
0
60
70
80
90
100
110
120
DAY
lev= 0.20 0.40 0.60 0.80 1.20 1.60 2.00
20
40
60
80
100
Biomass fraction(%)
Day of Year 2001 (JST)

Fig.3

a) March 20, 2001 0900JST (Jday 79)

b) March 21, 2001 0900JST (Jday 80)

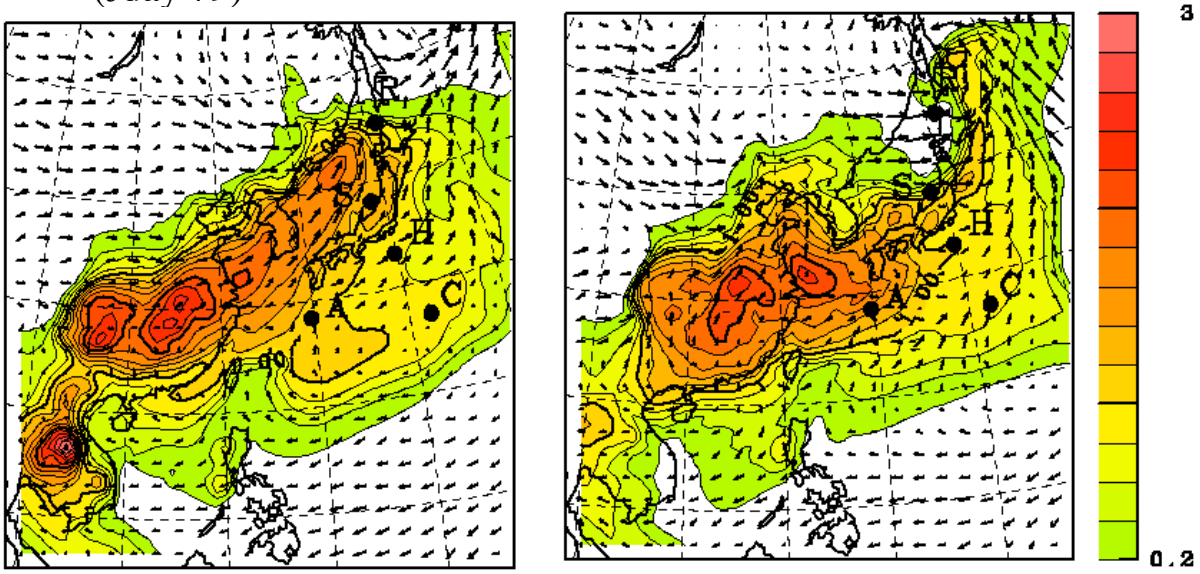

c) April 9, 2001 0900JST (Jday 99)

d) April 11, 2001 0900JST (Jday 101)

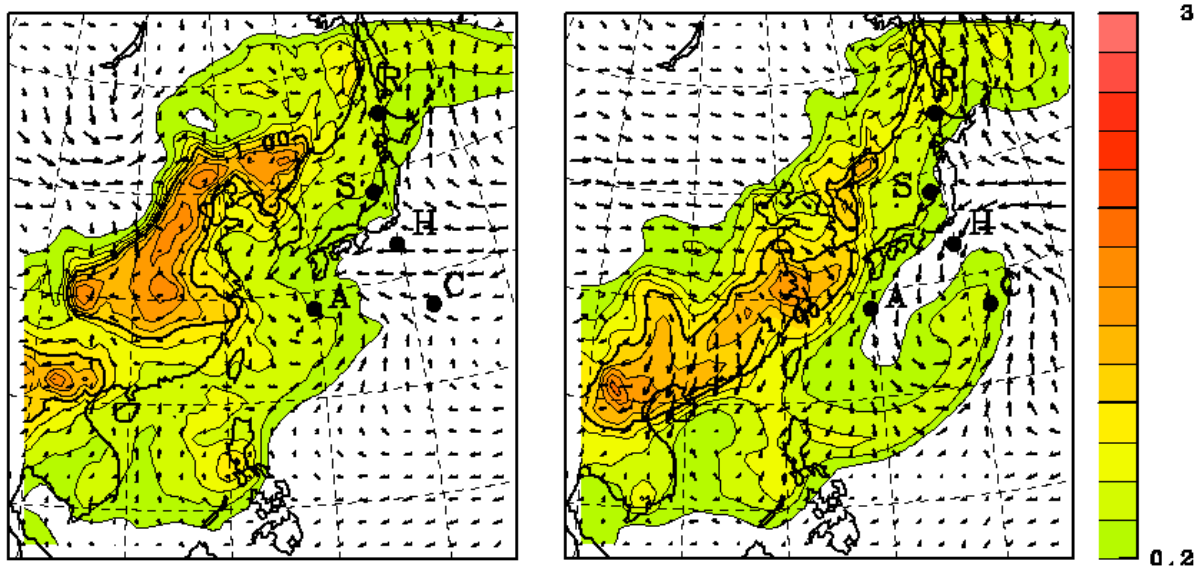

Fig.4

a) Surface BC concentration, horizontal Flux and BIOfrac

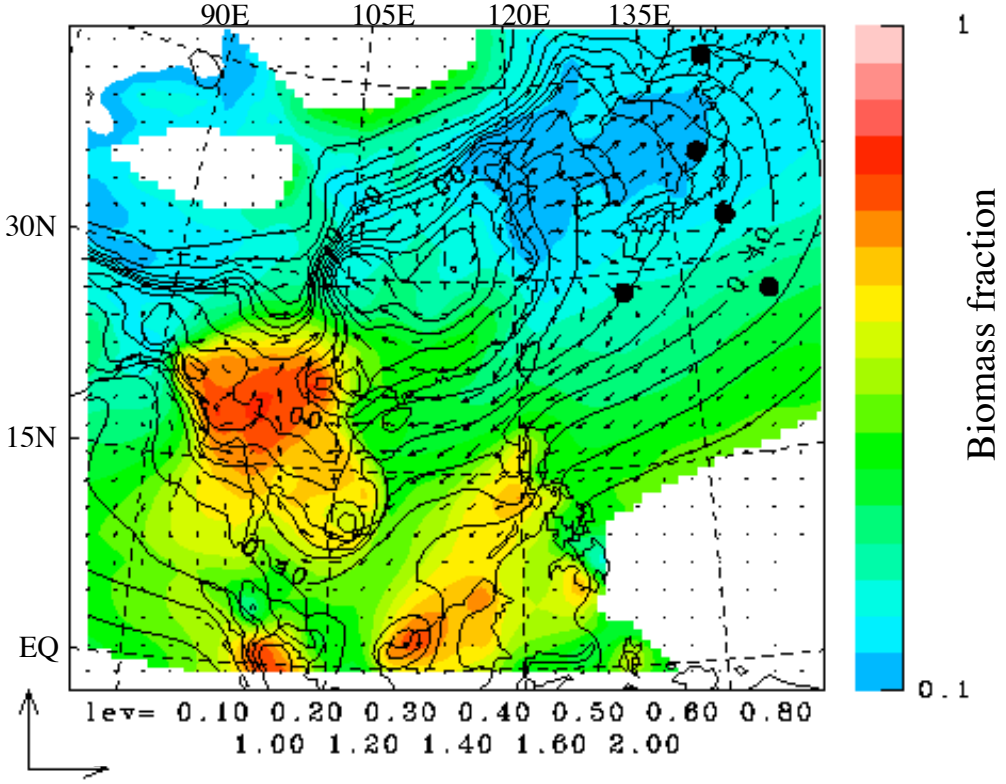

b) Column averaged Horizontal Flux and BIOfrac

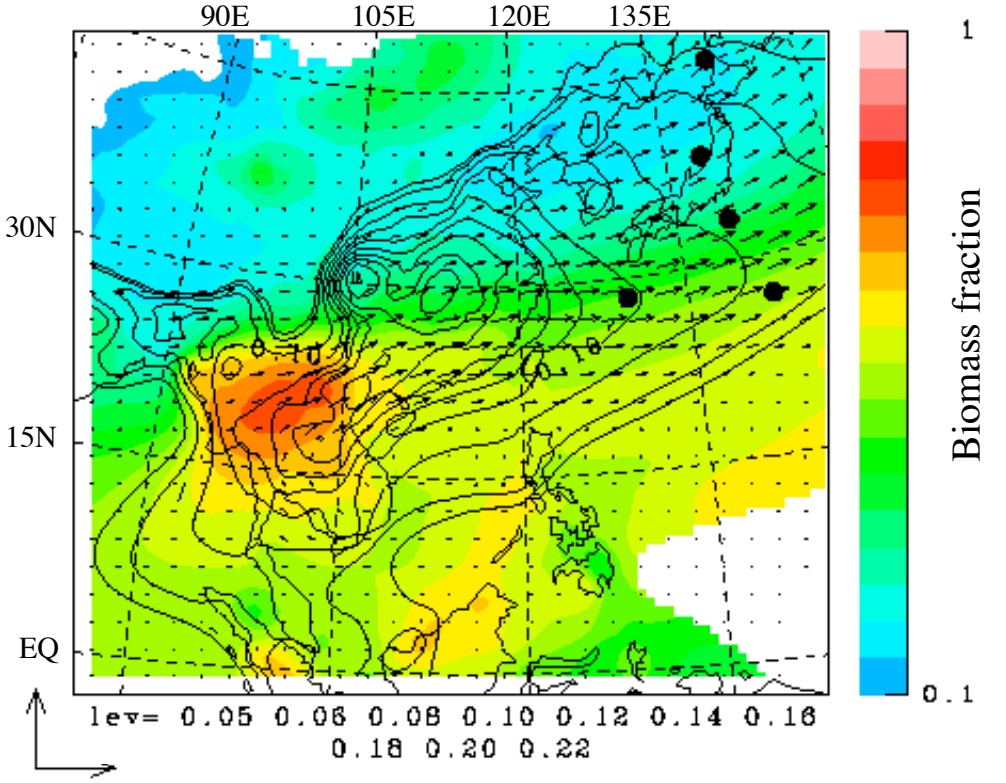

Fig.5

a) Averaged BC concentration and BIOfrac at 140°E

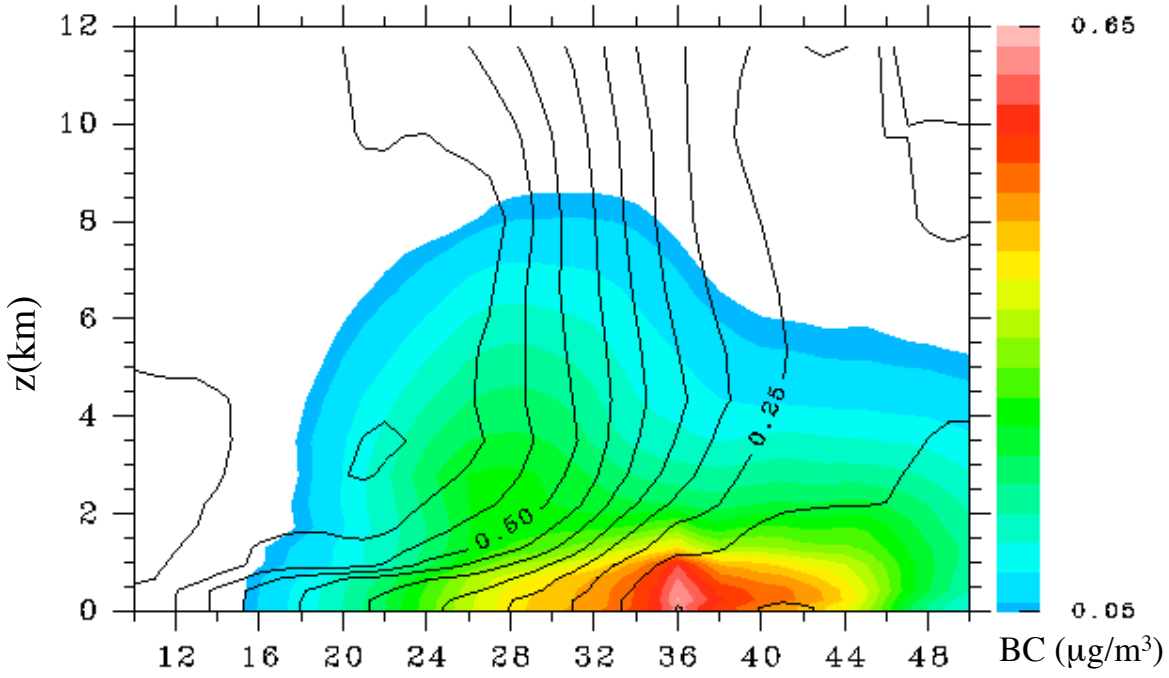

b) Averaged BC horizontal flux and BIOfrac at 140°E

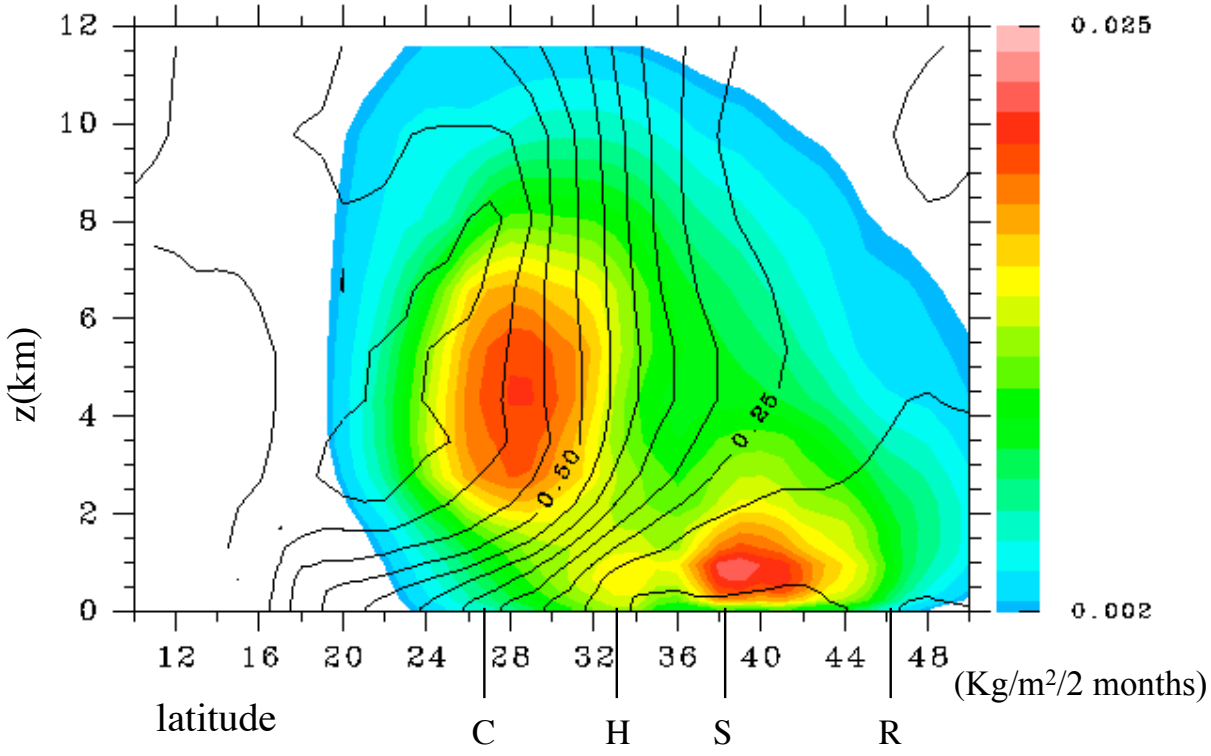

Fig.6

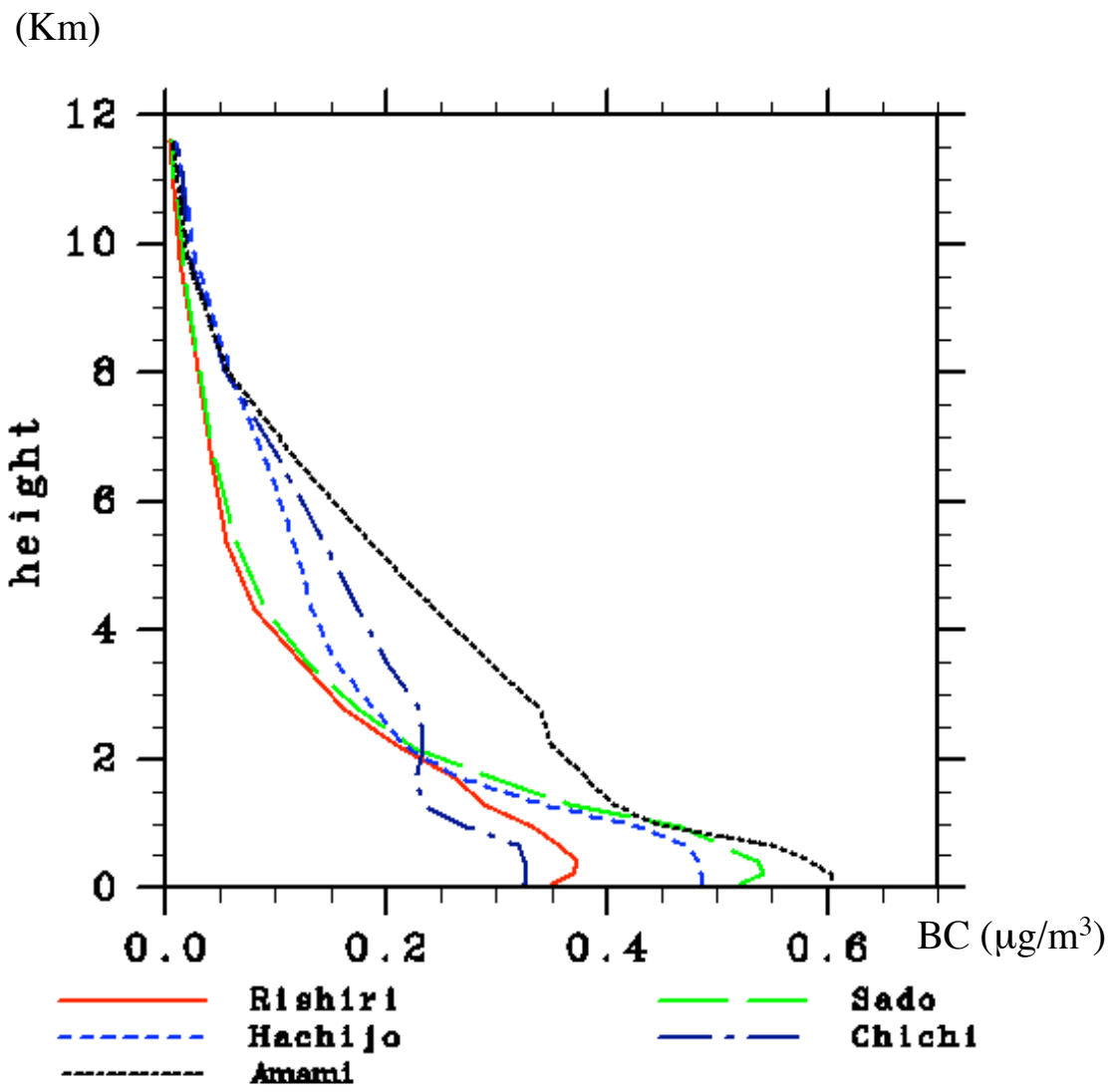
(Km)
height
12
10
8
6
4
2
0
0.0
0.2
0.4
0.6
BC (μg/m3)
Rishiri
Hachijo
Amami
Sado
Chichi

Fig. 7